Oxygen-related defects in low phosphorous content $GaAs_{1-y}P_y$ grown by metal organic vapor phase epitaxy

J. G. Cederberg,[a] K. L. Bray, and T. F. Kuech
Department of Chemical Engineering, University of Wisconsin, Madison, Wisconsin 53706

(Received 3 March 1997; accepted for publication 21 April 1997)

The mixed Group V ternary alloy $GaAs_{1-y}P_y$ ($y<0.17$) has been grown by metal organic vapor phase epitaxy and doped with oxygen using the oxygen precursor, diethylaluminum ethoxide [$C_2H_5OAl(C_2H_5)_2$]. Controlled oxygen doping was accomplished over the range of $0<y<0.17$. Deep level transient spectroscopy measurements reveal the presence of several oxygen-related deep levels. These levels, previously found in GaAs:O, vary with alloy composition over the investigated range. An additional deep level, most probably associated with the presence of misfit-related defects, has been identified. Photoluminescence performed on the oxygen-doped samples indicates that band edge emission is reduced and lower energy emission features are introduced over the wavelength range of 1000–1200 nm as a result of oxygen incorporation. © *1997 American Institute of Physics.* [S0021-8979(97)06714-5]

I. INTRODUCTION

$GaAs_{1-y}P_y$ alloys have been used extensively for light emitting diodes (LEDs) in the red and orange spectral regions. Due to this wide use, several investigations of the electrical and optical characteristics of $GaAs_{1-y}P_y$ have been performed on materials grown by a variety of techniques.[1–3] One impurity common to all growth techniques is oxygen. Oxygen-induced deep levels in binary compound semiconductors, especially GaAs and GaP, have been studied in depth.[4,5] In GaP, electrically active oxygen is known to occupy a site of tetrahedral symmetry, substituting for phosphorus.[4] The lattice location of oxygen in GaAs is less well defined. Studies on GaAs, grown by the liquid encapsulated Czochralski (LEC) or horizontal Bridgman (HB) techniques, assign an off-center substitutional site, O_{As}, to electrically active oxygen.[5] Electrically inactive oxygen resides in an interstitial site.[5]

The effect of oxygen on $GaAs_{1-y}P_y$ has not been as thoroughly studied as in its component binaries.[6] Changing the composition of the alloy provides a means by which the effect of the microscopic environment on the defect characteristics can be determined. Some investigations have been performed on the energy position of the oxygen level over the range of $GaAs_{0.35}P_{0.65}$ to GaP using photoluminescence spectroscopy.[6] Extrapolation of this data, obtained for a high phosphorous content $GaAs_{1-y}P_y$, has assigned a level of $E_c-E_t=0.79$ eV for the O_{As} defect in GaAs. The work reported here presents results of deep level transient spectroscopy (DLTS) and growth studies of oxygen-related defects in low phosphorous content $GaAs_{1-y}P_y$ ($x<0.17$). When combined with existing data,[6] a complete picture of the nature of the oxygen defect in $GaAs_{1-y}P_y$ alloys over the entire composition range is obtained.

II. EXPERIMENT

Samples of $GaAs_{1-y}P_y$ were grown in a horizontal, low pressure (78 Torr) reactor in a hydrogen carrier gas at 600 °C with a V/III~100. Trimethylgallium (TMGa), arsine (AsH_3), and phosphine (PH_3) were used as growth precursors. Disilane, diluted to 10 ppm in hydrogen, was used for *n*-type doping. Oxygen was incorporated using the molecular dopant source diethylaluminum ethoxide (DEAlO). DEAlO has been shown to be effective in doping many III-V compound semiconductors such as GaAs,[7] InP,[8] and $In_xGAa_{1-x}As$.[8] DEAlO incorporates oxygen through a strong Al–O bond. The electrically active oxygen in GaAs:O, grown using DEAlO, has been assigned to defect complexes in which one or more Al atoms occupy Ga sites and O resides at or near the arsenic site.[5]

Double crystal x-ray diffraction (DCXRD) was performed on thick (~2 μm) relaxed samples to determine the layer composition. The composition was determined from Vegard's law using peak splittings from the rocking curves. The solid phase composition ($y=n_P/(n_p+n_{As})$, where n is the molar density of the specified element) is plotted in Fig. 1 as a function of the fraction of PH_3 in the group V feed to the reactor ($x=PH_3$ partial pressure/total group V partial pressure). At a growth temperature of 600 °C, the distribution coefficient for phosphorous, i.e., the ratio of y to x, for $GaAs_{1-y}P_y$ is less than unity. This behavior has been reported previously for the growth of $GaAs_{1-y}P_y$,[9] as well as other phosphorous-based alloys,[10] when using PH_3. Samples were grown using a step-graded buffer layer to reduce the dislocation density resulting from the lattice mismatch between the epilayer and the GaAs substrate. The buffer layer was formed by increasing the solid phase phosphorous composition by $\Delta y=0.02$ for every 50 nm of growth until the desired composition was reached. A thick layer of constant composition was then grown on the buffer layer structure. This method produced a generally specular surface morphology with a two dimensional crosshatch pattern.

The doping characteristics of DEAlO in $GaAs_{1-y}P_y$ were studied through the growth of multilayer samples. Layers, each 0.5 μm in thickness, were grown in which step changes in the DEAlO mole fraction were made while holding the disilane mole fraction and alloy composition con-

[a]Electronic mail: cederber@quiche.che.wisc.edu

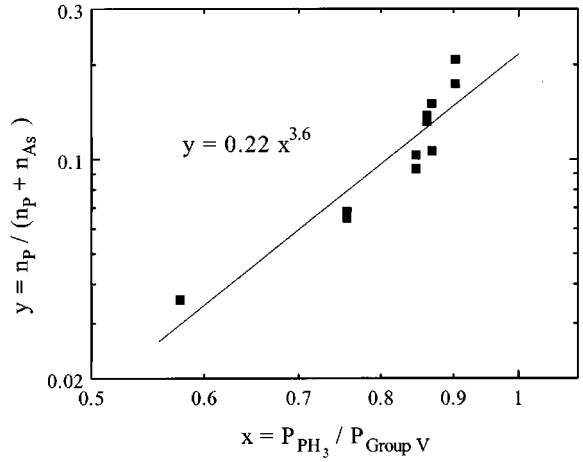

FIG. 1. The phosphorus mole fraction in the epilayer (y) was determined by DCXRD as a function of the fraction of PH_3 in the group V feed. Resulting distribution coefficient (y/x) is less than unity as noted in previous studies (Refs. 9 and 10).

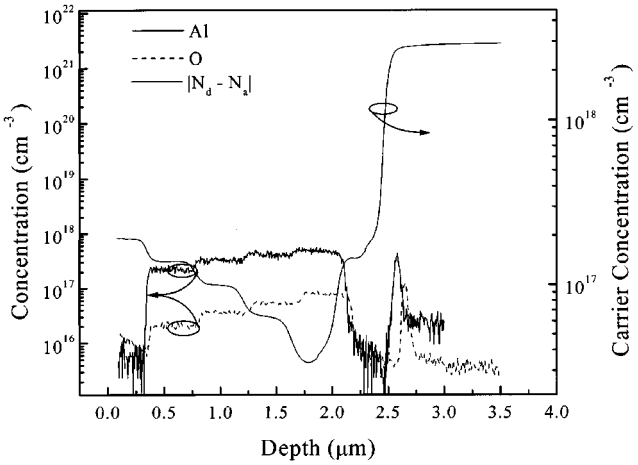

FIG. 2. SIMS and EC–V profiles for a multilayer $GaAs_{0.9}P_{0.1}$ sample where the gas phase DEAlO mole fraction was changed stepwise during growth. The left axis is the concentration of oxygen and aluminum, as determined by SIMS, and the right axis is the free-carrier concentration. The silicon concentration is constant at 2×10^{7} cm^{-3}.

stant. Two types of quantitative information about the doping characteristics of DEAlO were obtained. Electrochemical capacitance–voltage (EC–V) measurements on these multilayer samples determined the net carrier concentration and the amount of compensation of shallow silicon donors introduced by oxygen. Secondary ion mass spectroscopy (SIMS) measurements were also used to determine the amount of oxygen and aluminum incorporated at a given DEAlO mole fraction.

Single layer samples of a constant alloy composition, silicon and oxygen concentration were grown for DLTS measurements. Comparison samples without oxygen doping were also grown. These samples allow separation of the oxygen-related signals from those due to possible lattice misfit-related defects. Schottky diodes were fabricated using electron beam evaporation to deposit a AuGe(12%)/Ni/Ti/Au (80/20/20/80 nm) ohmic contact. Au Schottky contacts (0.19 mm^2) were subsequently defined using optical lithography and formed by electron beam evaporation. DLTS measurements were carried out using a reverse bias of -1 V pulsing to 0 V for 1 ms unless otherwise stated. Capacitance–voltage (C–V) measurements were also performed on the Schottky diodes for trap concentration calculations.

Photoluminescence (PL) spectroscopy was performed on the DLTS samples at 12 K using the 514 nm line of an Ar^+ laser for excitation, with a power density of 1.25 W/cm^2. The signal was dispersed by a 1 m single monochromator and the signal was detected with either a photomultiplier tube, with a sensitivity range from 560 to 1100 nm, or a liquid nitrogen cooled Ge detector, which is sensitive from 750 to 1800 nm.

III. RESULTS

A. Doping studies

The EC-V and SIMS profiles for a $GaAs_{0.9}P_{0.1}$ sample codoped with Si and DEAlO are shown in Fig. 2. Step increases in the DEAlO mole fraction introduced during growth result in a stepwise decrease in the carrier concentration. This decrease in electron concentration indicates that oxygen behaves as an electron trap. In the absence of any incorporated oxygen, the electron concentration would be constant throughout the layer, at a value of 2×10^{17} cm^{-3}. Doping level amounts of aluminum are also incorporated with the oxygen as measured by SIMS. In GaAs, doped using DEAlO, the Al and O form a defect complex, which is responsible for the observed electrical behavior.[7] From the EC-V and SIMS results, a comparison of the oxygen incorporation behavior into $GaAs_{1-y}P_y$ can be drawn relative to that of GaAs. In the case of GaAs doped with DEAlO, the oxygen concentration dependence on the DEAlO gas phase mole fraction is described by a power law relationship. Such a power law relationship is shown in Fig. 3 for the concentration of oxygen, aluminum, and free-carrier compensation ($n_{\text{no oxygen}}-n_{\text{oxygen}}$) as a function of the gas phase DEAlO mole fraction for $GaAs_{0.9}P_{0.1}$ [Fig. 3(a)] and $GaAs_{0.83}P_{0.17}$ [Fig. 3(b)]. A comparison of the exponents from the power law fit indicates that oxygen incorporation from DEAlO is less efficient as PH_3 is introduced into the growth environment.[11] However, the total amount of compensation introduced increases slightly as the amount of phosphorus incorporated increases. Table I summarizes the results from Fig. 3 for GaAs and the alloy. Instead of the strong, superlinear dependence observed for GaAs, oxygen incorporation more closely follows a linear dependence on the DEAlO mole fraction, while aluminum incorporation is slightly superlinear. In general, the amount of oxygen incorporated into $GaAs_{1-y}P_y$ alloys is less than that incorporated into GaAs for the same DEAlO mole fraction.[11] Under the same conditions, with a V/III ratio of 100 and a growth temperature of 600 °C, an oxygen concentration of 6×10^{19} cm^{-3} in GaAs is expected for a DEAlO mole fraction of 2×10^{-6}.[11] This is compared to oxygen concentrations in $GaAs_{1-y}P_y$ of 5×10^{16} cm^{-3} for $y=0.1$, and 2×10^{16} cm^{-3} for $y=0.17$, for the same gas phase DEAlO mole fraction and V/III ratio.

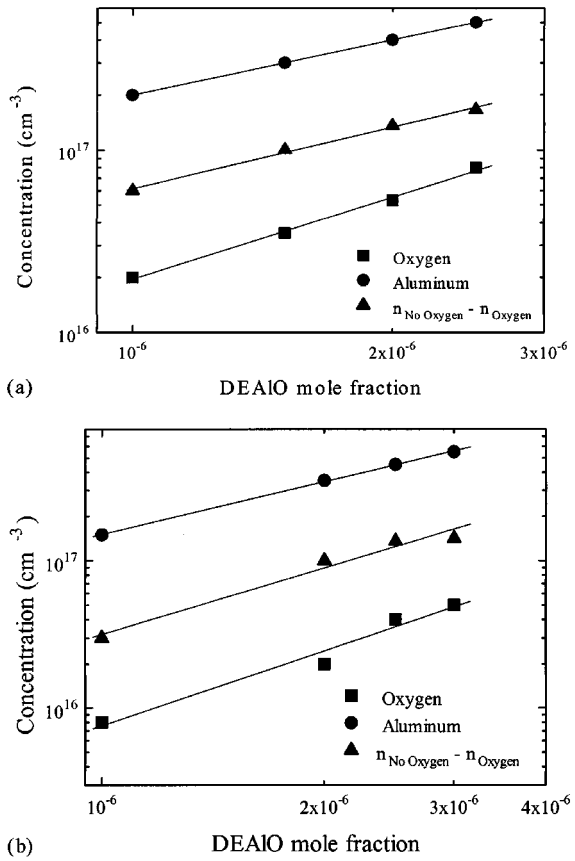

FIG. 3. Plots of oxygen, aluminum, and electron trap concentrations vs gas phase DEAlO mole fraction for (a) $GaAs_{0.9}P_{0.1}$ and (b) $GaAs_{0.83}P_{0.17}$. The data was fit to a power law expression of the form Concentration α (DEAlO mole fraction).[11] Exponents determined from these regressions are shown in Table I.

TABLE I. Power law exponents (n) for $GaAs_{1-x}P_x$ and GaAs for the curve fits shown in Fig. 3.

	GaAs	$GaAs_{0.9}P_{0.1}$	$GaAs_{0.83}P_{0.17}$
Oxygen	~4	1	1.2
Aluminum	1	1.5	1.7
$n_{\text{No Oxygen}} - n_{\text{Oxygen}}$	2	1	1.5

B. Electrical characterization

Single layer samples were characterized by E$C-V$, and oxygen and aluminum concentrations were determined from the multilayer SIMS profiles. Table II presents the physical and electrical data for the samples studied in this investigation. Samples 1 and 4 were the control samples, doped only with Si. Additional codoped samples were grown under identical conditions using disilane and DEAlO. All samples contained a 0.3 μm Si-doped buffer layer (2×10^{17} cm^{-3}) under the codoped layer, allowing the direct measurement of the electrical compensation.

Typical DLTS spectra for samples 2 ($GaAs_{0.9}P_{0.1}$:Si:O) and 6 ($GaAs_{0.83}P_{0.17}$:Si:O), which had comparable amounts of oxygen, along with their respective control samples are given in Fig. 4. The $GaAs_{0.9}P_{0.1}$:Si control sample (sample 1) only has a single, small peak, labeled E1 in Table II, which is detected at 225 K for the rate window shown. We will attribute and refer to this peak as resulting from the presence of misfit dislocations or other misfit-related defects, based on the results of this study as discussed below. In sample 2 ($GaAs_{0.9}P_{0.1}$:Si:O), two emission peaks were detected over the measurement range. The peak centered around 375 K is considered to be the major peak found in GaAs:Si:O shifted toward higher temperatures. A second peak is detected near 160 K. Multiple oxygen-related peaks were also previously found in the DLTS spectra of GaAs:Si:O.[7] A third sample (sample 3) containing a higher oxygen concentration was found to have a similar DLTS spectrum to the lower doped sample (sample 2). The misfit-related defects can be seen as shoulders in the DLTS spectra of the $GaAs_{0.9}P_{0.1}$:Si:O samples. The DLTS signal intensity of the misfit-related peak was too small in these samples to adequately characterize its energy level and concentration.

As the composition of phosphorus in the alloy is increased, the major oxygen-related DLTS peaks are shifted toward higher temperatures. Determination of the higher energy peaks required either a longer rate window or higher measurement temperatures. Such experimental conditions were not accessible in this study, due to limitations in the DLTS system and the degradation of the Schottky diode at high temperatures. In sample 4 ($GaAs_{0.83}P_{0.17}$:Si), the amplitude of the peak attributed to misfit dislocations increased and an additional peak appeared as a low temperature shoulder on this peak. In the spectrum for sample 6 ($GaAs_{0.83}P_{0.17}$:Si:O), the misfit related peak is now superimposed on the oxygen related defect, affecting the determination of the peak position. This composite peak in the spectrum was fitted with two, superimposed Gaussian functions to determine the characteristic peak temperature and the peak height. In the $GaAs_{0.83}P_{0.17}$:Si control sample, defect E1, which is attributed to misfit dislocations, lies at 0.38 eV below the conduction band. For $GaAs_{0.83}P_{0.17}$:Si:O, the misfit-related peak is also found after the composite peak is separated by regression, and the calculated energy level is very close to the 0.38 eV determined for this defect in $GaAs_{0.83}P_{0.17}$:Si. Also, the measured defect concentrations for the defect E1 are constant for all $GaAs_{0.83}P_{0.17}$ samples, within our measurement uncertainty, indicating that the defect is not due to DEAlO. Typical Arrhenius plots of the experimentally determined emission rates for $GaAs_{0.9}P_{0.1}$:Si:O and $GaAs_{0.83}P_{0.17}$:Si:O are shown in Figs. 5 and 6, respectively. All peak energies are referenced to the conduction band edge. The highest energy peak, labeled E2 in Table II, has shifted 54 meV to an average of 0.80 eV in $GaAs_{0.90}P_{0.10}$ from its position in GaAs of 0.75 eV.[7] As the alloy composition is shifted to $GaAs_{0.83}P_{0.17}$, this peak energy level further increases to an average value of 0.82 eV. Lastly, defect E3, near 0.34 and 0.26 eV in material with $y=0.10$ and $y=0.17$, respectively, appears only in material doped with DEAlO.

It should be noted that the total number of defects measured by DLTS is approximately one order of magnitude less than the total amount of compensation measured by EC-V. Also, the effect of incomplete trap filling has been accounted for in our data analysis.[12] This difference between DLTS-

TABLE II. Physical and electrical data for samples used in this study.

Sample	Composition	$\lvert N_d-N_a\rvert$ (cm^{-3}) $\times 10^{16}$	$\Delta\lvert N_d-N_a\rvert$ (cm^{-3}) $\times 10^{16}$	[O] (cm^{-3}) $\times 10^{16}$ (est.)	[Al] (cm^{-3}) $\times 10^{16}$ (est.)	E_c-E_t (eV)	σ_t (cm^2) $\times 10^{-14}$ (from intercept)	N_t (cm^{-3}) $\times 10^{14}$
1	$GaAs_{0.9}P_{0.1}$:Si	20	⋯	⋯	⋯	E1 0.412±0.005	7±2	1.4
2	$GaAs_{0.9}P_{0.1}$:Si:O	6	7.7	3.6	30	E2 0.833±0.007	70±20	80±30
						E3 0.353±0.005	50±10	19±7
3	$GaAs_{0.9}P_{0.1}$:Si:O	5.5	12.1	5.5	40	E2 0.775±0.005	14±2	70±10
						E3 0.324±0.005	11±2	13±1
4	$GaAs_{0.83}P_{0.17}$:Si	20	⋯	⋯	⋯	E1 0.381±0.005	1.6±0.3	6±2
						E4 0.173±0.005	0.008±0.001	1.1±0.3
5	$GaAs_{0.83}P_{0.17}$:Si:O	18	11	2.5	50	E1 0.346±0.005	0.2±0.03	4.0±0.8
						E2 0.800±0.007	12±3	40±10
						E3 0.269±0.005	0.1±0.4	3.7±0.8
6	$GaAs_{0.83}P_{0.17}$:Si:O	15	19	3.4	55	E1 0.302±0.005	0.026±0.004	4.2±0.3
						E2 0.837±0.007	23±5	72.5±11.9
						E3 0.256±0.005	0.08±0.02	9.5±2.0

measured trap concentration and total compensation indicates the presence of at least one other defect at a significant concentration deeper in the energy gap.

The pulse width was varied from 0.1 to 10 ms to determine if the measured traps were saturated during the voltage pulse. The magnitude of the signal varied ±15% for the oxygen-related peaks, with no clear trends, indicating that these traps were saturated during the filling pulse. The misfit dislocation-related peaks did show an increase in the DLTS emission signal with an increased pulse width, indicating the presence of a small capture barrier. The characteristics of the misfit dislocation-related peak was not studied further.

C. Optical characterization

PL spectroscopy was carried out at 12 K on the samples used in the DLTS measurements. The near-visible spectral features obtained from the $GaAs_{0.9}P_{0.1}$ and $GaAs_{0.83}P_{0.17}$ samples are given in Fig. 7. The Si only control samples possessed peaks at 769 nm (1.61 eV) and 756 nm (1.64 eV), in Figs. 7(a) and 7(b), respectively, which are associated with band-to-band recombination. These peak positions lead to band gap energies and compositions which agree with the compositions as determined by DCXRD.[13] There is an additional feature at about 1000 nm in the Si only control

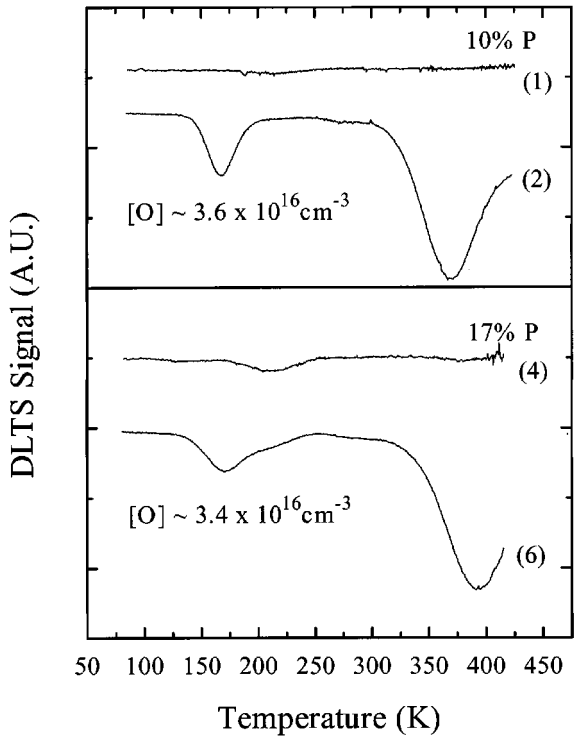

FIG. 4. A characteristic DLTS spectra for the samples studied. Samples were measured at a reverse bias of −1 V, pulsing to 0 V for 1 ms. The period used was 500 ms with a rate window of 21.5 ms. The sample designations are given on the figure and correspond to those in Table II.

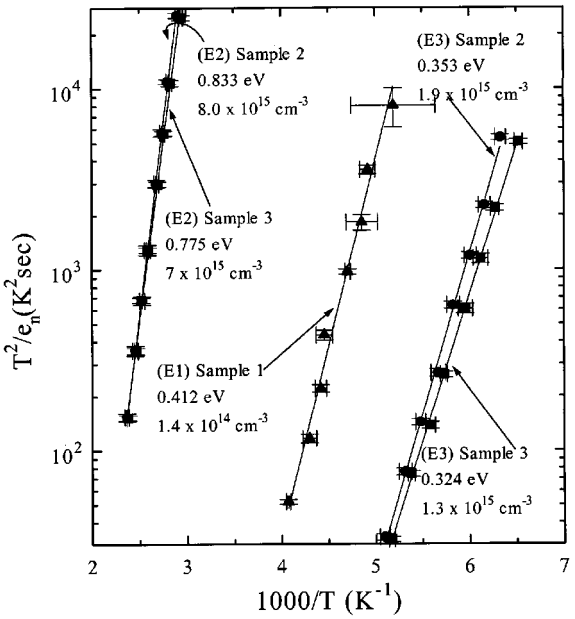

FIG. 5. Arrhenius plot of the emission rates for the measured deep levels in $GaAs_{0.9}P_{0.1}$:Si:O, grown using DEAlO (■, ●) as well as the Si only control sample (▲).

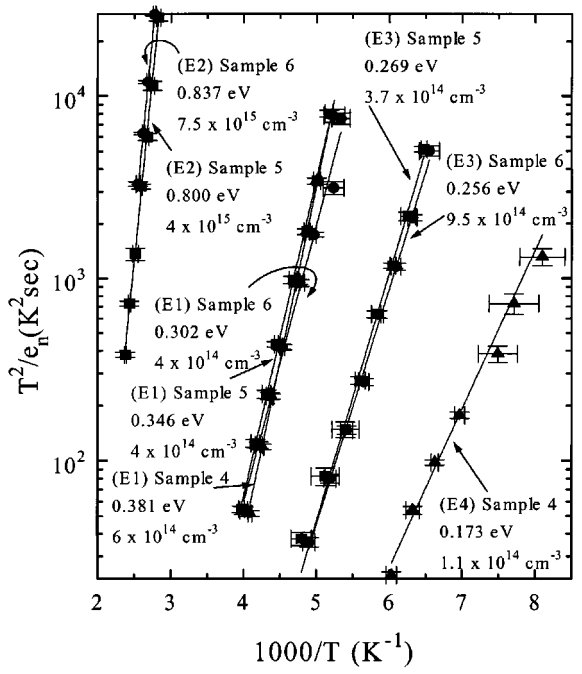

FIG. 6. Arrhenius plot of the emission rates for the measured deep levels in $GaAs_{0.83}P_{0.17}$:Si:O, grown using DEAlO (■, ●) as well as the Si only control sample (▲).

samples. This peak has previously been attributed to a $Si–V_{Ga}$ defect complex in GaAs and GaP.[14–17]

The near-band edge PL features are dramatically reduced with increasing oxygen concentration in the oxygen-containing samples. New spectral features also appear as oxygen is incorporated into the alloy in both the near-band edge and at longer wavelengths. The deep infrared spectra for the silicon and silicon and oxygen codoped $GaAs_{0.9}P_{0.1}$ and $GaAs_{0.83}O_{0.17}$ samples are shown in Fig. 8. The dominant long wavelength spectral features are centered around 1000 and 1200 nm. The 1000 nm peak grows with increasing oxygen concentration and is superimposed on the $Si–V_{Ga}$ peak found in the control samples. Additionally, peaks attributed to V_{Ga}-O_p ,[18,19] as well as group IV–V_{Ga},[20] complexes have been noted in the near-band edge luminescence of GaP. A peak at 1200 nm has been previously seen in GaAs:O.[21] These infrared peaks are also seen in GaAs:Si:O but at lower energies.[22] The intensities of these peaks increase with the amount of oxygen incorporated. The intensity of these peaks also increase with excitation power, with the higher energy peak increasing at a faster rate.

IV. DISCUSSION

The oxygen incorporation from DEAlO during GaAs growth has been studied in detail.[11,23] From previous as phase decomposition studies, the gas phase decomposition of DEAlO proceeds through the sequential loss of C_2H_4 via a β-hydride elimination reaction, forming $(C_2H_5)_{2-x}H_xAlOC_2H_5$ in the gas phase.[11] Such species can form gas phase adducts with Lewis bases, i.e., PH_3 and AsH_3, which are in excess in the gas phase. The formation of this gas phase adduct preserves the oxygen-containing compounds from additional decomposition, resulting in enhanced transport to the growth front. This mechanism has been used to explain the dependence of both the aluminum and oxygen incorporation into GaAs:O from DEAlO and explains the strong V/III ratio dependence previously seen in the oxygen doping of GaAs.[11] Similar reactions are expected in the

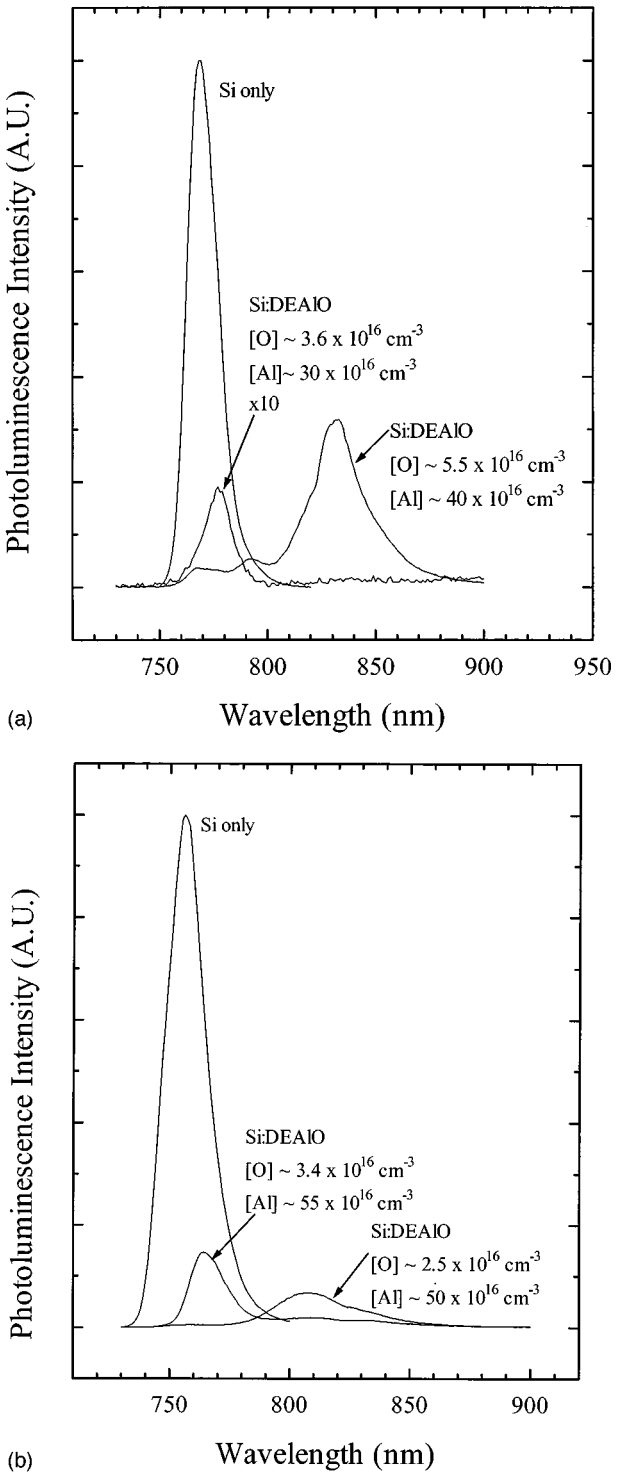

FIG. 7. Near visible photoluminescence spectra for (a) $GaAs_{0.9}P_{0.1}$ and (b) $GaAs_{0.83}P_{0.17}$ samples which contained either no oxygen or varying amounts of incorporated oxygen. The band edge emission is reduced with the incorporation of oxygen in all cases with the appearance of additional lower energy luminescence peaks.

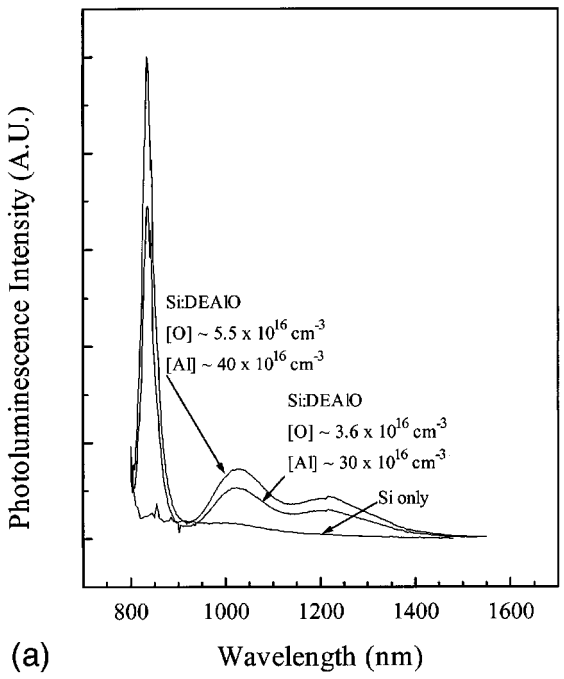

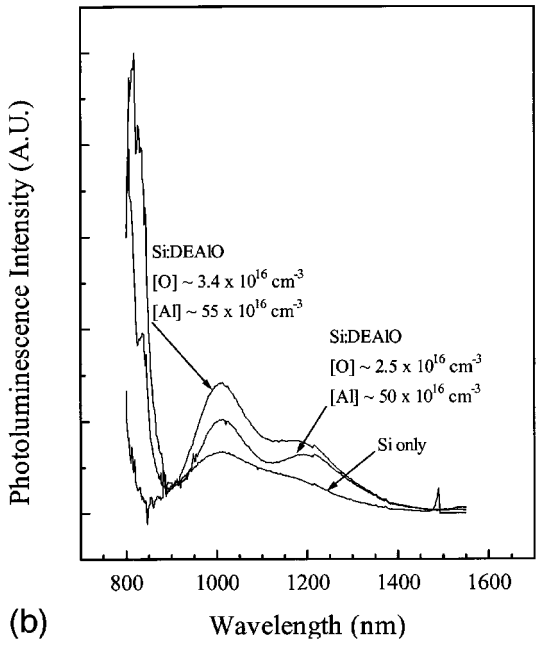

FIG. 8. Deep infrared photoluminescence spectra for (a) $GaAs_{0.9}P_{0.1}$ and (b) $GaAs_{0.83}P_{0.17}$ indicate several deep luminescence features clearly associated with oxygen incorporation. Similar peaks have been found in GaAs:O samples (Ref. 21).

present case where there is a great excess, in the gas phase, of both PH_3 and AsH_3. The oxygen incorporation efficiency into $GaAs_{1-y}P_y$ from DEAlO is different, in detail, from the case of GaAs:O. Some general trends of nonlinear incorporation of oxygen and aluminum with increasing DEAlO mole fraction are observed indicating that the general features of the gas phase chemistry should be unchanged. It should be noted that there is a competing process in oxygen doping with DEAlO which is the formation of H_2O from the H_2 carrier gas and hydride sources, at the growth front, that

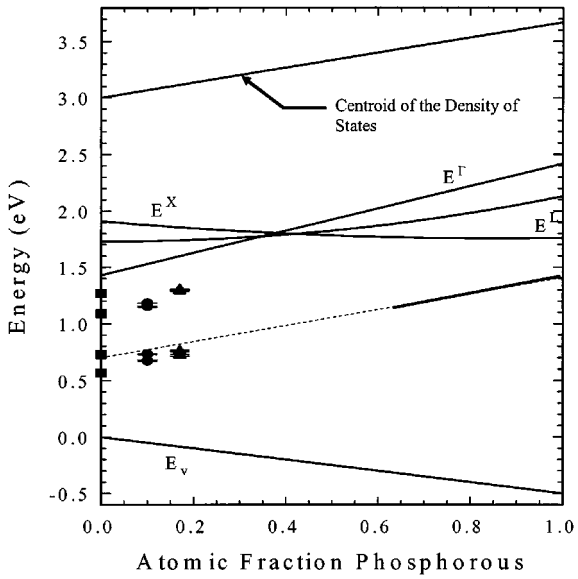

FIG. 9. The oxygen related defect energy levels are presented as a function of the alloy composition assuming the GaAs valence band as the energy reference. The valence band discontinuity between GaAs and GaP is assumed to be linear with values obtained from Ref. 30. Major features of band structure are plotted for the reference. The solid curve at high P-contents represent data from the previous work of Wolford, *et al.* (Ref. 6). The data presented for GaAs:O were obtained from the work of Huang, *et al.* (Ref. 7).

subsequently can desorb, leaving aluminum on the surface. The complexities of the competing gas phase reactions prevent the determination of the specific major reaction pathway in this combined AsH_3–PH_3 system leading to the incorporation of oxygen.

The effect of misfit dislocations on the electrical properties of semiconductors has been investigated, and it is known that they can introduce states within the energy gap.[24] Since $GaAs_{1-y}P_y$ is not lattice matched to the GaAs substrate, these dislocation-related defects are present in our samples. The defect E1 in $GaAs_{0.83}P_{0.17}$ is attributed to misfit dislocations. This assignment is supported by the composition dependence of the defect concentration measured by DLTS and the fact that the defect concentrations are independent of oxygen concentration within the uncertainty of our measurements.

As mentioned above, the defects introduced into GaAs by DEAlO have been studied in depth. Five defect levels are reported for GaAs doped with a comparable amount of oxygen.[7] Only two of the five defects detected in GaAs:Si:O were detected in $GaAs_{1-y}P_y$Si:O within the measurement sensitivity. Level E2 is believed to be the 0.75 eV level detected in GaAs. This is deduced from its position in the temperature spectrum and its comparable capture cross section (σ_t). As phosphorus is added to the crystal, this level is pushed further down in the band gap, going from an average value of 0.80 eV in $GaAs_{0.9}P_{0.1}$ to 0.82 eV in $GaAs_{0.83}P_{0.17}$. Another level is detected in DEAlO-doped samples with an energy position varying from an average of 0.34 eV for $GaAs_{0.9}P_{0.1}$ to 0.26 eV for $GaAs_{0.83}P_{0.17}$. This shallower level is also more localized as indicated from the estimated capture cross section of 0.15×10^{-14} cm^2 for $GaAs_{0.83}P_{0.17}$.

This level may be related to the 0.24 eV level seen in GaAs, which has a capture cross section of 0.15×10^{-14} cm^2.[7] The presence of multiple PL and DLTS peaks may indicate that oxygen is present in several atomic configurations. Oxygen is paired with one or more aluminum atoms, and the number of nearest neighbor aluminum atoms may change the ionization energy of the defect.[25] Unlike the GaAs case, there is the possibility of a variation in the second-nearest neighbor shell surrounding the defect. This is due to the possible statistical variation in the average number of As and P atoms in this shell. Since this shell is composed of 12 atoms, the primary influence of the variation from $y=0$ to 0.17 in $GaAs_{1-y}P_y$ is expected to be the change in the overall band structure of the host material since the site-to-site variation of the oxygen should be small.

A large discrepancy exists between the amount of compensation as observed by EC–V and the calculated trap concentrations. In GaAs:Si:O, a deep level is seen at 0.86 eV. An additional, deeper trap in $GaAs_{1-y}P_y$, outside of our measurement range, would explain this observed discrepancy.

The oxygen-induced energy levels determined by DLTS are plotted as a function of composition in Fig. 9. The energy position deduced from the PL peak position for phosphorous-rich $GaAs_{1-y}P_y$ ($y>0.65$) implanted with oxygen is plotted along with a proposed linear extrapolation to the position of the oxygen-related defect in GaAs.[6] The principal levels determined in this study agree quite well with this simple linear extrapolation from the previously reported values. Deviation from this linear extrapolation may be attributed to the variation in the energy level position of oxygen due to the coincorporation of Al. Previous studies on deep levels have proposed different theories concerning the relationship of the specific band structure features to the defect deep level energy and electronic structure.[26–28] It has been proposed that localized defects, like oxygen, are linked to the bulk of the electronic states.[27] In Fig. 9, the centroid of the conduction band density of states is plotted, assuming a linear interpolation with composition.[29] Defect E2 appears to track the bulk of the electronic states, not the vacuum level or a particular band edge as proposed for some deep impurities.

This present study has determined several deep levels associated with the presence of oxygen in $GaAs_{1-y}P_y$. The position of these oxygen-related electronic states qualitatively agree with the previous extrapolation of the oxygen defect in high phosphorus-content $GaAs_{1-y}P_y$.[6] When combined with these previous measurements, this present study completes the determination of the oxygen defect throughout this technologically important alloy system.

V. CONCLUSIONS

This study has investigated the incorporation of oxygen-related defects into $GaAs_{1-y}P_y$ using the oxygen-containing precursor, DEAlO. The study indicates that the amount of oxygen incorporated into the alloy is reduced as compared to GaAs for the same gas phase DEAlO mole fraction. DLTS has been used to measure the position of the oxygen related defects in approximately the upper half of the band gap. Comparison of the results with data taken for the high phosphorous content $GaAs_{1-y}P_y$ indicate that the oxygen-related defect may follow the bulk of the conduction band states and not a vacuum reference level. PL measurements show that the incorporation of oxygen reduces band-to-band luminescence and introduces new features in the infrared region.

ACKNOWLEDGMENTS

The authors would like to acknowledge support for the Army Research Office and the National Science Foundation. Jen-Wu Huang and Steven Stockman of Hewlett Packard Corp. are gratefully acknowledged for assisting with SIMS analysis used in this work.

[1] E. Callega, E. Munoz, and F. Garcia, Appl. Phys. Lett. **42**, 428 (1983).
[2] M. G. Craford, G. E. Stillman, N. Holonyak, Jr. and J. A. Rossi, J. Electron. Mater. **20**, 3 (1989).
[3] P. Omling, L. Samuelson, and H. G. Grimmeiss, J. Appl. Phys. **54**, 5117 (1983).
[4] P. Dean, in *Deep Centers in Semiconductors*, edited by S. T. Pantelides, 2nd ed. (Gordon and Breach, Philadelphia, 1993), p. 227.
[5] M. Skowronski, in *Deep Centers in Semiconductors*, edited by S. T. Pantelides, 2nd ed. (Gordon and Breach, Philadelphia, 1993), p. 389.
[6] D. J. Wolford, S. Modesti, and B. G. Streetman, Inst. Phys. Conf. Ser. **65**, 501 (1983).
[7] J. W. Huang and T. F. Kuech, Appl. Phys. Lett. **65**, 604 (1994).
[8] J.-W. Huang, T. F. Kuech, and T. J. Anderson, Appl. Phys. Lett. **67**, 1116 (1995); J. W. Huang and T. F. Kuech, 7th Biennial Workshop on Organometallic Vapor Phase Epitaxy, Ft. Myers, FLA, April 2–6, 1995 (unpublished).
[9] T. Fukui and N. Kobayashi, J. Cryst. Growth **71**, 9 (1985).
[10] S. Pellegrino and L. Vitali, J. Electron. Mater. **25**, 519 (1996).
[11] J. W. Huang, D. F. Gaines, T. F. Kuech, R. M. Potemski, and F. Cardone, J. Electron. Mater. **23**, 659 (1994).
[12] D. Stievenard and D. Vuillaume, J. Appl. Phys. **60**, 973 (1986).
[13] B. J. Steetman, *Solid State Electronic Devices*, 4th ed. (Prentice-Hall, London, 1995), p. 223.
[14] E. W. Williams, Phys. Rev. **168**, 922 (1968).
[15] C. J. Hwang, J. Appl. Phys. **40**, 4584 (1969).
[16] D. T. J. Hurle, J. Phys. Chem. Solids **40**, 627 (1979).
[17] M. Holtz, T. Stauncy, T. Dallas, and S. Massie, Phys. Rev. B **50**, 14 706 (1994).
[18] R. N. Bharagava, S. K. Kurtz, A. T. Vink, and R. C. Peters, Phys. Rev. Lett. **27**, 183 (1971).
[19] P. J. Dean, Solid State Commun. **9**, 2211 (1971).
[20] J. M. Dishman, D. F. Daly, and W. P. Knox, J. Appl. Phys. **43**, 4593 (1972).
[21] J. M. Ryan, J.-W. Huang, T. F. Kuech, and K. L. Bray, J. Appl. Phys. **76**, 1175 (1994).
[22] J. M. Ryan, J.-W. Huang, T. F. Kuech, and K. L. Bray (unpublished).
[23] S. Nayak, J. W. Huang, J. M. Redwing, D. E. Savage, M. G. Lagally, and T. F. Kuech, Appl. Phys. Lett. **68**, 1270 (1996).
[24] H. F. Matare, *Defect Electronics in Semiconductors* (Wiley-Interscience, New York, 1971), p. 222.
[25] T. F. Kuech, S. Nayak, J.-W. Huang, and J. Li, J. Cryst. Growth **163**, 171 (1996).
[26] H. Hasegawa and H. Ohno, Jpn. J. Appl. Phys. **25**, 1319 (1986).
[27] P. M. Mooney, J. Appl. Phys. **67**, R1 (1990).
[28] T. Hasizume, H. Hasegawa, and H. Ohno, J. Appl. Phys. **68**, 3394 (1990).
[29] Landolt-Bornstein, *Numerical Data and Functional Relationships in Science and Technology* (Springer, Berlin, 1982), Vol. 103, pp. 45, 49.
[30] E. Yu, J. O. McCaldin, and T. C. McGill, Solid State Phys. **46**, 1 (1993).